ASCL2 reciprocally controls key trophoblast lineage decisions during hemochorial placenta development

Kaela M. Varberg[a,b,1], Khursheed Iqbal[a,b], Masanaga Muto[a,b], Mikaela E. Simon[a,b], Regan L. Scott[a,b], Keisuke Kozai[a,b], Ruhul H. Choudhury[c,d], John D. Aplin[c,d], Rebecca Biswell[e], Margaret Gibson[e], Hiroaki Okae[f], Takahiro Arima[f], Jay L. Vivian[a,b], Elin Grundberg[b,e,g], and Michael J. Soares[a,b,g,h,i,1]

[a]Institute for Reproduction and Perinatal Research, University of Kansas Medical Center, Kansas City, KS 66160; [b]Department of Pathology and Laboratory Medicine, University of Kansas Medical Center, Kansas City, KS 66160; [c]Maternal and Fetal Health Research Centre, Institute of Human Development, The University of Manchester, Manchester M13 9WL, United Kingdom; [d]Academic Health Science Centre, St Mary's Hospital, Manchester M13 9WL, United Kingdom; [e]Center for Pediatric Genomic Medicine, Children's Mercy Research Institute, Kansas City, MO 64108; [f]Department of Informative Genetics, Environment and Genome Research Center, Tohoku University Graduate School of Medicine, 980-8575 Sendai, Japan; [g]Center for Perinatal Research, Children's Mercy Research Institute, Kansas City, MO 64108; [h]Department of Pediatrics, University of Kansas Medical Center, Kansas City, KS 66160; and [i]Department of Obstetrics and Gynecology, University of Kansas Medical Center, Kansas City, KS 66160

Edited by R. Michael Roberts, University of Missouri, Columbia, MO, and approved January 27, 2021 (received for review August 4, 2020)

Invasive trophoblast cells are critical to spiral artery remodeling in hemochorial placentation. Insufficient trophoblast cell invasion and vascular remodeling can lead to pregnancy disorders including preeclampsia, preterm birth, and intrauterine growth restriction. Previous studies in mice identified achaete-scute homolog 2 (ASCL2) as essential to extraembryonic development. We hypothesized that ASCL2 is a critical and conserved regulator of invasive trophoblast cell lineage development. In contrast to the mouse, the rat possesses deep intrauterine trophoblast cell invasion and spiral artery remodeling similar to human placentation. In this study, we investigated invasive/extravillous trophoblast (EVT) cell differentiation using human trophoblast stem (TS) cells and a loss-of-function mutant *Ascl2* rat model. *ASCL2* transcripts are expressed in the EVT column and junctional zone, which represent tissue sources of invasive trophoblast progenitor cells within human and rat placentation sites, respectively. Differentiation of human TS cells into EVT cells resulted in significant up-regulation of *ASCL2* and several other transcripts indicative of EVT cell differentiation. Disruption of ASCL2 impaired EVT cell differentiation, as indicated by cell morphology and transcript profiles. RNA sequencing analysis of ASCL2-deficient trophoblast cells identified both down-regulation of EVT cell-associated transcripts and up-regulation of syncytiotrophoblast-associated transcripts, indicative of dual activating and repressing functions. ASCL2 deficiency in the rat impacted placental morphogenesis, resulting in junctional zone dysgenesis and failed intrauterine trophoblast cell invasion. ASCL2 acts as a critical and conserved regulator of invasive trophoblast cell lineage development and a modulator of the syncytiotrophoblast lineage.

trophoblast | invasion | placenta | differentiation

To accommodate increased fetal nutrient and oxygen demands during gestation, uterine spiral arteries are remodeled into distended, low-resistance vessels (1). Central to the remodeling process are invasive or extravillous trophoblast (EVT) cells (2). Invasive trophoblast cells enter and transform the uterus by establishing residence between blood vessels and supplanting the endothelium, where they adopt a pseudoendothelial cell phenotype (2–4). If trophoblast cell invasion and vascular remodeling are insufficient, pregnancy disorders such as preeclampsia, preterm birth, and intrauterine growth restriction can develop and threaten both maternal and fetal health (5, 6). The goal of this study was to integrate in vitro and in vivo models to identify critical and conserved mechanisms of invasive trophoblast cell lineage development.

The mouse, although successfully used to study some features of placentation, exhibits shallow trophoblast cell invasion and is not an optimal model for investigating the trophoblast-uterine interface (3, 7, 8). In contrast, the rat has deep intrauterine trophoblast cell invasion and spiral artery remodeling similar to human placentation (9, 10). In the rat, the invasive trophoblast cell lineage arises from progenitors located in the junctional zone, a structure analogous to the EVT column of the human placenta (11, 12). Conservation between rat and human hemochorial placentation serves as the foundation of our research approach (10, 13).

Regulatory mechanisms of invasive trophoblast cell development and function are largely unknown. Previous studies in the mouse identified achaete-scute family bHLH transcription factor 2 (ASCL2) as essential to extraembryonic development, particularly in spongiotrophoblast and trophoblast giant cell formation (14–19). ASCL2 is expressed as early as the preimplantation blastocyst stage in trophectoderm cells, with robust expression also present postimplantation in the ectoplacental cone and subsequently in spongiotrophoblast cells (14, 20). Disruption of mouse ASCL2 results in embryonic lethality around midgestation (14, 21). ASCL2 is one of several genes located within

Significance

Defective placentation, including impaired uterine spiral artery remodeling, leads to pregnancy disorders such as pregnancy loss, preeclampsia, intrauterine growth restriction, and preterm birth, all of which cause significant morbidity and mortality for the mother and fetus. Trophoblast cells are central to executing placental functions and can differentiate into two conserved specialized lineages: invasive/extravillous trophoblast cells, which guide uterine transformation, and syncytiotrophoblast, which serve a barrier function. We leveraged model systems to identify achaete-scute homolog 2 as a conserved regulator of the invasive/extravillous trophoblast cell lineage and a modulator of the syncytiotrophoblast phenotype. A key upstream regulator of trophoblast-engineered uterine transformation has been identified representing an entry point into the etiology of pregnancy complications resulting from defective placentation.

Author contributions: K.M.V., K.I., M.M., J.L.V., and M.J.S. designed research; K.M.V., K.I., M.M., M.E.S., R.L.S., K.K., R.B., M.G., and M.J.S. performed research; R.H.C., J.D.A., H.O., T.A., and E.G. contributed new reagents/analytic tools; K.M.V., K.I., E.G., and M.J.S. analyzed data; and K.M.V. and M.J.S. wrote the paper.

The authors declare no competing interest.

This article is a PNAS Direct Submission.

Published under the PNAS license.

[1]To whom correspondence may be addressed. Email: kvarberg@kumc.edu or msoares@kumc.edu.

This article contains supporting information online at https://www.pnas.org/lookup/suppl/doi:10.1073/pnas.2016517118/-/DCSupplemental.

Published March 1, 2021.

Downloaded at Palestinian Territory, occupied on December 11, 2021

www.manaraa.com

the imprinted domain on mouse chromosome 7 that have been associated with early developmental events (16, 22). Mechanisms regulating *Ascl2* imprinting within this domain have been investigated previously (17, 19, 22–24). ASCL2 has also been implicated in human trophoblast cell development (25–28) as a hypoxia-induced transcription factor that inhibits syncytiotrophoblast aromatase gene expression (29, 30). Recent reports using single-cell RNA sequencing (RNA-seq) technologies to discern distinct cell populations at the maternal-fetal interface in human tissues have confirmed ASCL2 expression in EVT cells (31, 32). Increasing evidence points to ASCL2 as a putative conserved regulator of trophoblast cell lineage development.

In the present study, we used in vitro and in vivo models to investigate the function of ASCL2 in trophoblast cell lineage development. In vitro studies using human and rat trophoblast stem (TS) cells provide insight into ASCL2 actions on trophoblast cell lineage development. In vivo studies using a loss-of-function mutant rat model have identified ASCL2 actions on trophoblast development in a physiological context. Our results indicate that ASCL2 is both critically important and highly conserved in invasive trophoblast/EVT cell lineage development. We provide insight into a dual-regulatory function of ASCL2 not only to promote invasive/EVT cell differentiation, but also to simultaneously suppress aspects of syncytiotrophoblast differentiation. Overall, ASCL2 acts as a key regulator determining trophoblast lineage cell fate.

Results

ASCL2 Expression in Invasive Trophoblast Cells Is Conserved in Hemochorial Placentation. Initially, we sought to verify the timing and localization of *ASCL2* expression in early human and rat placentation. Using in situ hybridization, we observed *ASCL2* expression within the EVT column of first trimester human tissue (Fig. 1 *A* and *B*). The EVT column is the site of invasive EVT progenitor cells in humans (Fig. 1*A*). Similarly, in early placentation in the rat (gestational day [gd] 12.5), we observed prominent *Ascl2* expression by in situ hybridization in the junctional zone, the site of invasive trophoblast progenitors (Fig. 1*B*), analogous to the EVT column in the human (Fig. 1*A*). *Ascl2* transcript levels progressively increase within uterine tissue proximal to the placenta throughout the second half of gestation in the rat (*SI Appendix*, Fig. S1). In first trimester human decidua, *ASCL2* transcripts colocalized with *HLA-G*, an extravillous trophoblast-specific transcript (Fig. 1*C*). This observed colocalization supports previous observations of *ASCL2* expression in human EVT (28). In the rat, *Ascl2* transcripts colocalized with *Prl7b1*, an invasive trophoblast cell-specific transcript (33), within the uterine parenchyma (Fig. 1*D*). *Ascl2* expression was especially prominent in endovascular invasive trophoblast cells. Thus, expression of ASCL2 by invasive trophoblast cells is conserved in human and rat hemochorial placentation.

ASCL2 Is Robustly Expressed in Human TS Cells Undergoing EVT Cell Differentiation. Human TS cells can be maintained in a highly proliferative stem state or readily differentiated into either invasive EVT or syncytiotrophoblast lineages (34). Cells cultured in stem state conditions divide and form discrete colonies with relatively homogeneous cobblestone morphology. Upon EVT cell differentiation, cells are transformed into elongated structures that are morphologically distinct from the stem state (*SI Appendix*, Figs. S2*A* and S3*A*). The morphological changes are accompanied by significant transcriptomic changes, including down-regulation of stem state-associated transcripts, such as Lin-28 homolog A (*LIN28A*), LDL receptor-related protein 2 (*LRP2*), and epithelial cell adhesion molecule (*EPCAM*), as well as up-regulation of known EVT cell-associated transcripts including major histocompatibility complex class I, G (*HLA-G*) and matrix metallopeptidase 2 (*MMP2*), as well as *ASCL2* (*SI Appendix*, Figs. S2*B* and S3*B*). Up-regulation of HLA-G is also robust at the protein level in EVT when visualized by immunofluorescence (*SI Appendix*, Fig. S2*C*). These observations were consistent across multiple human TS cell lines (*SI Appendix*, Fig. S3). Thus, the in vitro human TS cell culture model can be successfully leveraged to gain insight into potential regulatory roles for ASCL2 in trophoblast cell lineage development.

ASCL2 Is Required for EVT Cell Differentiation. We hypothesized that ASCL2 is a critical regulator of invasive trophoblast cell lineage development. To test our hypothesis, we used a loss-of-function approach to determine whether ASCL2 is required for EVT cell differentiation. *ASCL2* was knocked down in undifferentiated human TS cells using a lentiviral-mediated short hairpin RNA (shRNA) approach. Following puromycin selection, undifferentiated human TS cells were exposed to culture conditions that promote EVT cell differentiation (34). *ASCL2* was diminished in the ASCL2 knockdown group after 8 d of EVT cell differentiation compared with control ($P < 0.0001$) (Fig. 2*A*). The effectiveness of ASCL2 knockdown was also validated by Western blot analysis (*SI Appendix*, Fig. S3*F*). ASCL2 disruption resulted in significant morphological differences associated with EVT cell differentiation (Fig. 2*B* and *SI Appendix*, Fig. S3*C*). Compared with the control shRNA group, which exhibited cell elongation, differentiated human TS cells transduced with lentivirus containing ASCL2-specific shRNA sequences failed to elongate. Consistent with the morphological observations, ASCL2 knockdown also resulted in failed up-regulation of several EVT cell-associated transcripts (*HLA-G*, *MMP2*, *IGF2*, *PCSK6*, and *SNAI1*) following differentiation (Fig. 2*A* and *SI Appendix*, Fig. S3*D*) and a failure to express HLA-G protein as assessed by immunofluorescence (Fig. 2*C*). Overall, *ASCL2* knockdown interfered with structural and molecular indices of EVT cell differentiation. These results indicate that ASCL2 is required for EVT cell differentiation.

ASCL2 Knockdown Alters the Human TS Cell Transcript Profile. To identify global changes in EVT cell gene expression, RNA-seq was performed and transcript profiles were determined for control human TS cells and ASCL2-depleted human TS cells following differentiation. In Fig. 3*A*, a volcano plot depicts transcript level fold changes and a heat map displays clustering of up-regulated (red) and down-regulated (blue) genes in control and ASCL2-depleted cell samples (Dataset S1). Consistent with morphologic observations and initial candidate assessments, we identified significant down-regulation of several EVT-specific transcripts, including *HLA-G*, *CCR1*, *NOTUM*, and *PLOD2* (Fig. 3*B* and *SI Appendix*, Fig. S3*D*). Unexpectedly, knockdown of ASCL2 resulted in a significant up-regulation of syncytiotrophoblast-specific transcripts, including *SDC1*, *CYP19A1*, *CGB5*, and *ADM* (Fig. 3*B* and *SI Appendix*, Fig. S3*E*). We used two- and three-dimensional methods for inducing syncytiotrophoblast differentiation (ST2D and ST3D) from human TS cells to compare with transcript expression up-regulated by ASCL2 knockdown. Expression of *SDC1* was comparable in ST2D, ST3D, and *ASCL2* knockdown cells, while *CYP19A1*, *ADM*, and *CGB5* expression levels were significantly increased as a result of ASCL2 knockdown but at lower levels than those seen in ST2D or ST3D differentiated cells (Fig. 3*D*).

Despite a strong syncytiotrophoblast signature in the list of up-regulated transcripts resulting from ASCL2 knockdown, we recognized the absence of some key syncytiotrophoblast markers, including the syncytins and their respective receptors (35). Knockdown of ASCL2 did not significantly affect the expression of syncytin-1 (*ERVW-1*) or syncytin-2 (*ERVFRD-1*), whereas syncytin-1 receptor (*SLC1A5*) and syncytin-2 receptor (*MFSD2*) were down-regulated (Fig. 3*E*). Therefore, ASCL2 represses part, but not all, of the program required to develop the syncytiotrophoblast lineage when TS cells are directed to EVT cell differentiation (Fig. 3*C*).

Downloaded at Palestinian Territory, occupied on December 11, 2021
www.manaraa.com

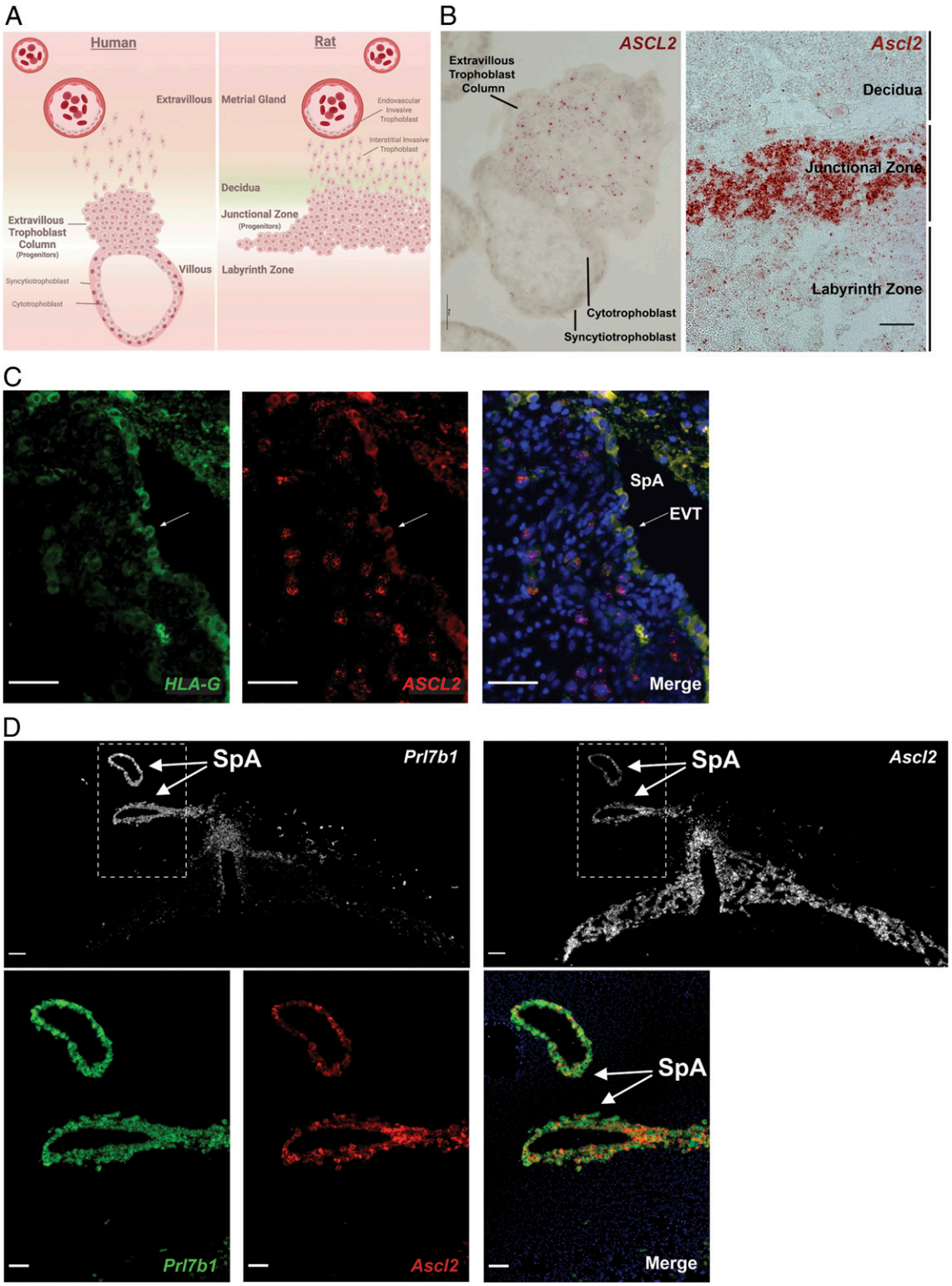

Fig. 1. *ASCL2* expression in invasive trophoblast cells is conserved in hemochorial placentation. (*A*) Schematic depicting the location of invasive trophoblast progenitor cells in human and rat. (*B*) Human placental tissue specimen obtained at 12 wk of gestation probed for *ASCL2* using in situ hybridization. *ASCL2* (red) is expressed in extravillous trophoblast column cells but not in syncytiotrophoblasts or cytotrophoblasts. Rat placental tissue specimen obtained from a gd 12.5 rat probed for *Ascl2* using in situ hybridization. *Ascl2* (red) is robustly expressed in the junctional zone compared with the decidua and labyrinth zones. (Scale bar, 50 μm.) (*C*) First trimester human uteroplacental tissue specimen probed for *HLA-G* (green) and *ASCL2* (red) using in situ hybridization. DAPI marks cell nuclei (blue). *HLA-G* is a known marker of EVT. The arrow indicates endovascular EVTs lining the decidual spiral arterioles (SpAs). (Scale bars, 50 μm.) (*D*) Rat placental tissue specimen obtained from a gd 12.5 rat probed for *Prl7b1* and *Ascl2* using in situ hybridization. (Scale bars, 200 μm.) Dotted lines depict the region shown below in higher magnification. DAPI marks cell nuclei (blue). *Prl7b1* (green) is a known marker of rat invasive trophoblast cells. Arrows indicate endovascular invasive trophoblast which line the decidual SpA. (Scale bars, 100 μm.)

Downloaded at Palestinian Territory, occupied on December 11, 2021

www.manaraa.com

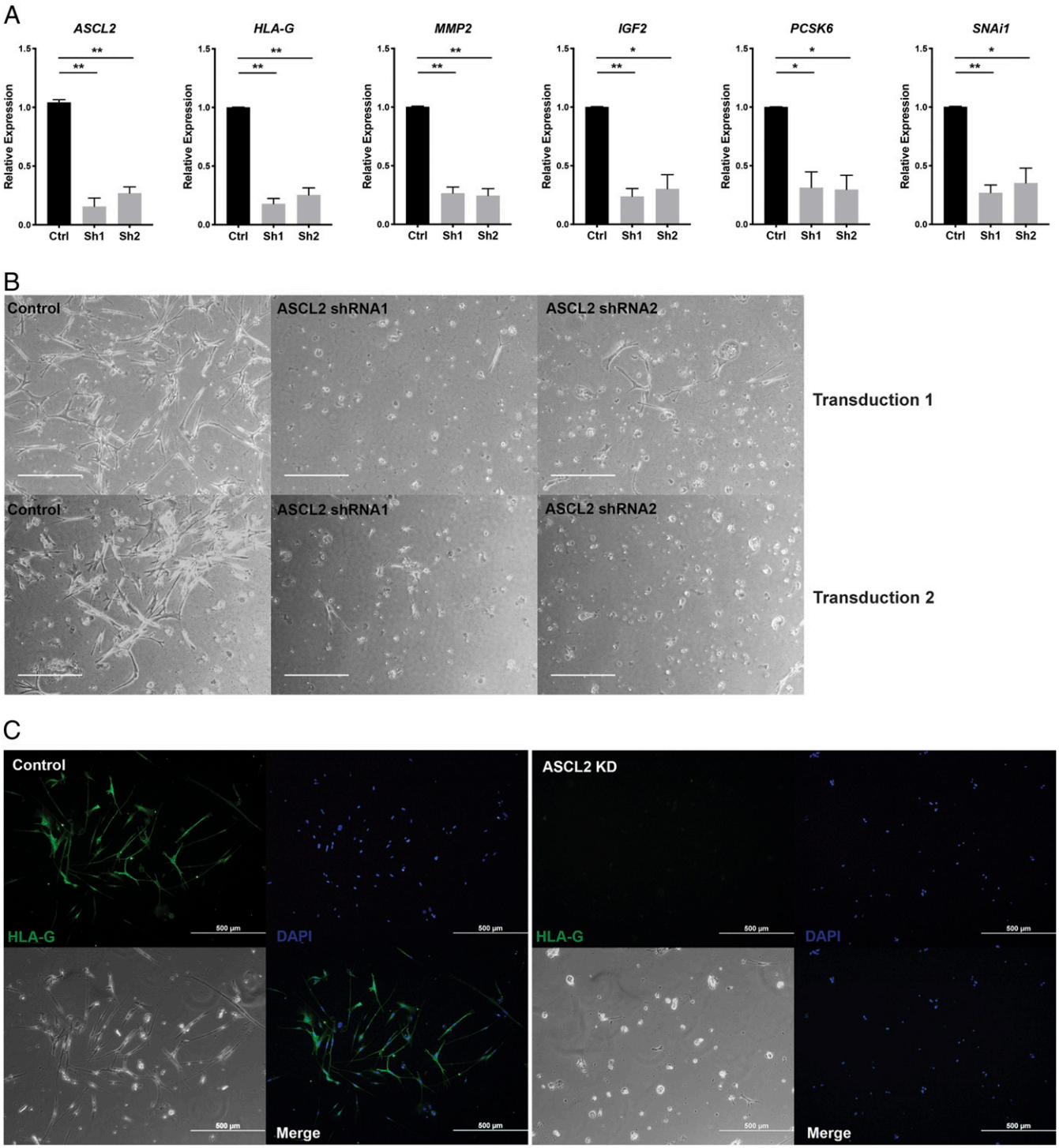

Fig. 2. ASCL2 is required for EVT differentiation. (*A*) Transcript levels of six invasive trophoblast markers (*ASCL2*, *HLA-G*, *MMP2*, *IGF2*, *PCSK6*, and *SNAI1*) on day 8 of EVT differentiation following transduction with lentivirus containing a control shRNA (Ctrl) or one of two independent ASCL2-specific shRNAs (Sh1 or Sh2). ASCL2 knockdown decreased levels of transcripts characteristic of invasive trophoblast cells ($n = 3$ transductions). $^{*}P < 0.05$; $^{**}P < 0.01$. All graphs depict means ± SD. (*B*) Phase-contrast images depicting cell morphology of EVT differentiated cells transduced with control shRNA (Control) or ASCL2-specific shRNA (ASCL2 shRNA 1 or 2) lentivirus on day 8 of EVT cell differentiation. (Scale bars, 500 μm.) (*C*) HLA-G (green) expression was evaluated in EVT differentiated cells on day 8 following transduction with lentivirus containing control shRNA (Control) or ASCL2-specific shRNA (ASCL2 KD) using immunocytochemistry. Phase-contrast images depict cell morphology, and DAPI labels cell nuclei. Merged fluorescence images overlay HLA-G and DAPI images. (Scale bars, 500 μm.)

Ascl2 Mutant Rats Exhibit Prenatal Lethality. We next sought to test the importance of ASCL2 in vivo and investigate potentially conserved mechanisms regulating hemochorial placentation. CRISPR/*Cas9* genome editing was used to generate an *Ascl2* null rat. A single guide RNA (gRNA) was designed to target the basic helix–loop–helix (bHLH) domain in exon 2 of the *Ascl2* gene

Downloaded at Palestinian Territory, occupied on December 11, 2021
www.manaraa.com

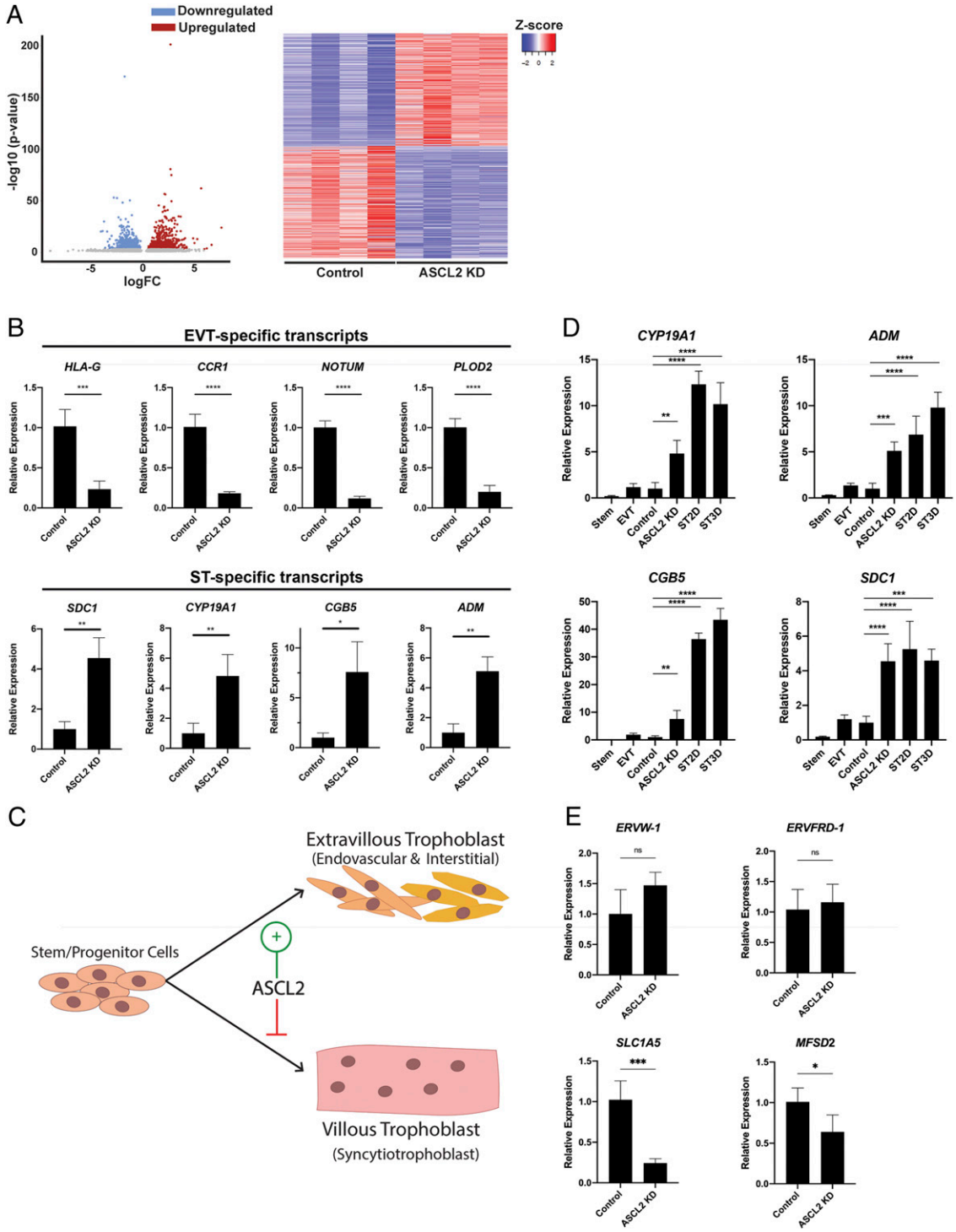

Fig. 3. ASCL2 knockdown alters the human TS cell transcript profile. (*A*) Volcano plot and heat map depicting RNA-seq analysis results of control (blue) and *ASCL2* shRNA-treated (red) EVT cells ($n = 4$ per group). Blue dots represent significantly down-regulated transcripts with $P \leq 0.05$ and a logarithm to base two-fold change of less than or equal to −2. Red dots represent significantly up-regulated transcripts with $P \leq 0.05$ and a logarithm to base two-fold change of ≥2. The heat map depicts difference in gene expression between four control and ASCL2 knockdown (KD) samples. The heat map color key represents *z*-scores of RPKM values. (*B*) Validation of RNA-seq results by qRT-PCR confirms that ASCL2 knockdown significantly decreases EVT-specific transcripts (*HLA-G*, *CCR1*, *NOTUM*, and *PLOD2*) and significantly increases syncytiotrophoblast (ST)-specific transcripts (*SDC1*, *CYP19A1*, *CGB5*, and *ADM*). $n = 4$ per group. $^{*}P < 0.05$; $^{**}P < 0.01$; $^{***}P < 0.001$; $^{****}P < 0.0001$. (*C*) Schematic depicting trophoblast cell differentiation from the stem/progenitor state toward either EVT cell or syncytiotrophoblast fates. (*D*) Relative expression of *CYP19A1*, *ADM*, *CGB5*, and *SDC1* in human TS cells cultured under the following conditions: stem state (Stem), following 8 d of EVT cell differentiation without transduction (EVT) or with transduction using control shRNA (Control) or ASCL2-specific shRNA (ASCL2 KD), or 6 d of syncytiotrophoblast differentiation using the ST2D or ST3D protocol (34). $n = 3$ to 4 per group. $^{**}P < 0.01$; $^{***}P < 0.001$; $^{****}P < 0.0001$. (*E*) Relative expression of *ERVW-1*, *ERVFRD-1*, *SLC1A5*, and *MFSD2* in human TS cells following 8 d of EVT cell differentiation with transduction using control shRNA (Control) or ASCL2-specific shRNA (ASCL2 KD). $n = 3$ to 4 per group. $^{*}P < 0.05$; $^{**}P < 0.01$; $^{****}P < 0.0001$. All graphs depict mean ± SD values.

Downloaded at Palestinian Territory, occupied on December 11, 2021

www.manaraa.com

(*SI Appendix*, Fig. S5*A*). A founder possessing a 247-bp deletion in exon 2, which is predicted to result in a frame shift and a premature stop codon before the bHLH domain, was selected for further experimentation (*SI Appendix*, Fig. S5*B*). Wild-type (WT; $^{+/+}$) and mutant ($^{-/-}$) PCR products (200 and 500 bp vs. 400 bp, respectively) are readily distinguishable for genotyping (*SI Appendix*, Fig. S5*C*). Breeding strategies were used to assess viability, litter composition, and imprinting in the *Ascl2* mutant rat strain. Inheritance of a maternal mutant *Ascl2* allele was associated with prenatal lethality, whereas offspring with a paternal mutant *Ascl2* allele were viable and fertile (*SI Appendix*, Fig. S6). Embryonic lethality occurred between gd 12.5 and gd 13.5 (*SI Appendix*, Fig. S7). In summary, disruption of the rat *Ascl2* gene results in phenotypic features similar to those previously reported for the mouse (14–19). *Ascl2* is paternally imprinted and essential for embryonic survival.

Ascl2 Mutant Placentation Sites Do Not Form an Intact Junctional Zone. The rat placenta is organized into two structurally and functionally well-defined compartments consisting of the junctional zone and the labyrinth zone. The junctional zone is situated at the interface with the uterus; is composed of a number of cellular constituents, including trophoblast giant cells, spongiotrophoblast cells, glycogen cells, and invasive trophoblast progenitor cells; and is homologous to the EVT column of the human placenta (Fig. 1*C*). The labyrinth zone connects the placenta to the fetus, provides an important barrier function, and is homologous to the villous compartment of the human placenta. These two placental compartments can be readily identified by gd 12.5 in the rat. Immunohistochemical assessment of vimentin staining at the rat maternal-fetal interface provides clear discernment of junctional and labyrinth zones. Using this approach, we determined that the *Ascl2* mutant placentas were smaller and lacked an intact junctional zone, unlike WT placentation sites (Fig. 4*A*).

Placental size differences prompted an analysis of cell proliferation in WT vs. *Ascl2* mutant placentation sites. Immunostaining for MKI67, a marker of cell proliferation, was widespread in the WT placenta but was more restricted in the *Ascl2* mutant placenta, with the most prominent expression occurring in trophoblast giant cells (Fig. 4*E*). *Mki67* transcript was significantly reduced in *Ascl2* mutant placentas compared with WT placentas (Fig. 4*F*). We used *Prl3d1* as a marker for trophoblast giant cells and found proportionally more trophoblast giant cells in *Ascl2* mutant placentation sites compared with WT placentation sites (Fig. 4*B*).

RNA-seq analysis was used to obtain additional insight into the involvement of ASCL2 in placental development (Fig. 4*C*). Transcript profiles exhibited profound differences in WT and *Ascl2* mutant gd 12.5 placentas (Fig. 4*C* and Dataset S2) and were indicative of a role for ASCL2 in the repression of trophoblast giant cell development (e.g., *Adm*, *Cyp11a1*, *Prl3d1*, *Hsd3b3*; Fig. 4*D*) and the activation of invasive trophoblast cell development (e.g., *Mmp15*, *Prl7b1*, *Ncam1*; Fig. 4*D*), but not labyrinth zone or syncytiotrophoblast lineage development.

Thus, ASCL2 is an essential regulator of the junctional zone compartment of the rat hemochorial placenta without an apparent effect on measures of labyrinth zone and syncytiotrophoblast lineage development.

Ascl2 and Rat TS Cell Differentiation. The above observations presented a potential species difference in the role of ASCL2 in the regulation of syncytiotrophoblast lineage development in the human versus the rat. However, a direct comparison of ASCL2's actions on syncytiotrophoblast development in human TS cells versus the rat placenta might not be optimal. Consequently, we investigated a role for ASCL2 in rat TS cell differentiation. Knockdown of ASCL2 resulted in up-regulation of transcripts associated with trophoblast giant cells (*Adm*, *Prl4a1*, *Pgf*, and *Cyp11a1*) and syncytiotrophoblast 1 (*Mct1*, *Glis1*, and *Stra6*) and syncytiotrophoblast 2 (*Gcm1*, *Synb*, and *Gcgr*) layers (*SI Appendix*, Fig. S4), with no evidence of invasive trophoblast cell development (e.g., failure of *Prl7b1* expression). These observations suggest that there may be some conservation in the inhibitory actions of ASCL2 on syncytiotrophoblast development; however, rat and human TS cells exhibit striking differences in vitro. Human TS cells can be induced to differentiate into EVT cells with an accompanying up-regulation of *ASCL2*, whereas conditions to promote invasive trophoblast cells have not been established for the rat. Rat TS cell differentiation is induced by mitogen removal and leads to a prominent down-regulation of *Ascl2* expression and primarily trophoblast giant cell differentiation (*SI Appendix*, Fig. S4). Additionally, different syncytiotrophoblast-associated transcripts are affected in human versus rat trophoblast cells. Although a perfect comparison between rat and human TS cells is not possible, it appears that ASCL2 may possess conserved actions inhibiting aspects of syncytiotrophoblast development.

Trophoblast Invasion Is Impaired in ASCL2-Deficient Placentation Sites. A key component of successful hemochorial placentation in the rat is deep trophoblast invasion and uterine spiral artery remodeling. Invasive trophoblast cells arise from progenitor cell populations within the junctional zone. Since *Ascl2* mutant placentation sites lack an intact junctional zone, we hypothesized that trophoblast cell invasion would be impaired. On gd 12.5, trophoblast cell invasion is restricted to the mesometrial decidua (Fig. 5*A*). At this gestational stage, invasion is limited to endovascular trophoblast cells lining decidual segments of uterine spiral arteries. We used immunofluorescence detection of cytokeratin to identify trophoblast cells within the mesometrial decidua of gd 12.5 WT and *Ascl2* mutant placentation sites. Endovascular invasive trophoblast cells were identified in WT, but not in *Ascl2* mutant, placentation sites (Fig. 5*B*).

We further supported these observations by examining transcripts specifically linked to invasive trophoblast cells in mesometrial decidua dissected from gd 12.5 placentation sites. *Prl7b1*, *Ncam1*, and *Mmp15* were significantly decreased in mesometrial decidua from *Ascl2* mutant compared with WT placentation sites (Fig. 5*C*). Furthermore, when we assessed *Ascl2* transcript localization by in situ hybridization in gd 12.5 WT placentation sites, we observed robust *Ascl2* expression in the junctional zone, as well as in endovascular trophoblast cells invading within the mesometrial decidua (Fig. 5*D*). Consequently, both progenitor and invasive trophoblast cell populations are affected in the *Ascl2* mutants.

In summary, ASCL2 is a key conserved driver of invasive trophoblast cell lineage development with reciprocal inhibitory actions on syncytiotrophoblast development.

Discussion

Placentation is an essential developmental process required for viviparity. Our current understanding of regulatory processes controlling placentation is fragmented. An established framework for elucidating biological processes includes dissection of biochemical events using cells in culture and complementary analyses testing the physiological importance of these same events using a relevant animal model. Most insight into the regulation of hemochorial placentation, as seen in both humans and rodents, is derived from an assortment of in vitro human trophoblast cell models and mouse mutagenesis. The relevance of many human trophoblast cell systems for investigating the EVT cell lineage is questionable (36–38), as is the use of the mouse for examination of the invasive trophoblast cell lineage (9). Implementation of human TS cells for experimental dissection of molecular mechanisms controlling EVT cell development (34, 39) and the rat for interrogation of regulatory processes controlling deep placentation (9, 10) offers scientifically robust

Downloaded at Palestinian Territory, occupied on December 11, 2021
www.manaraa.com

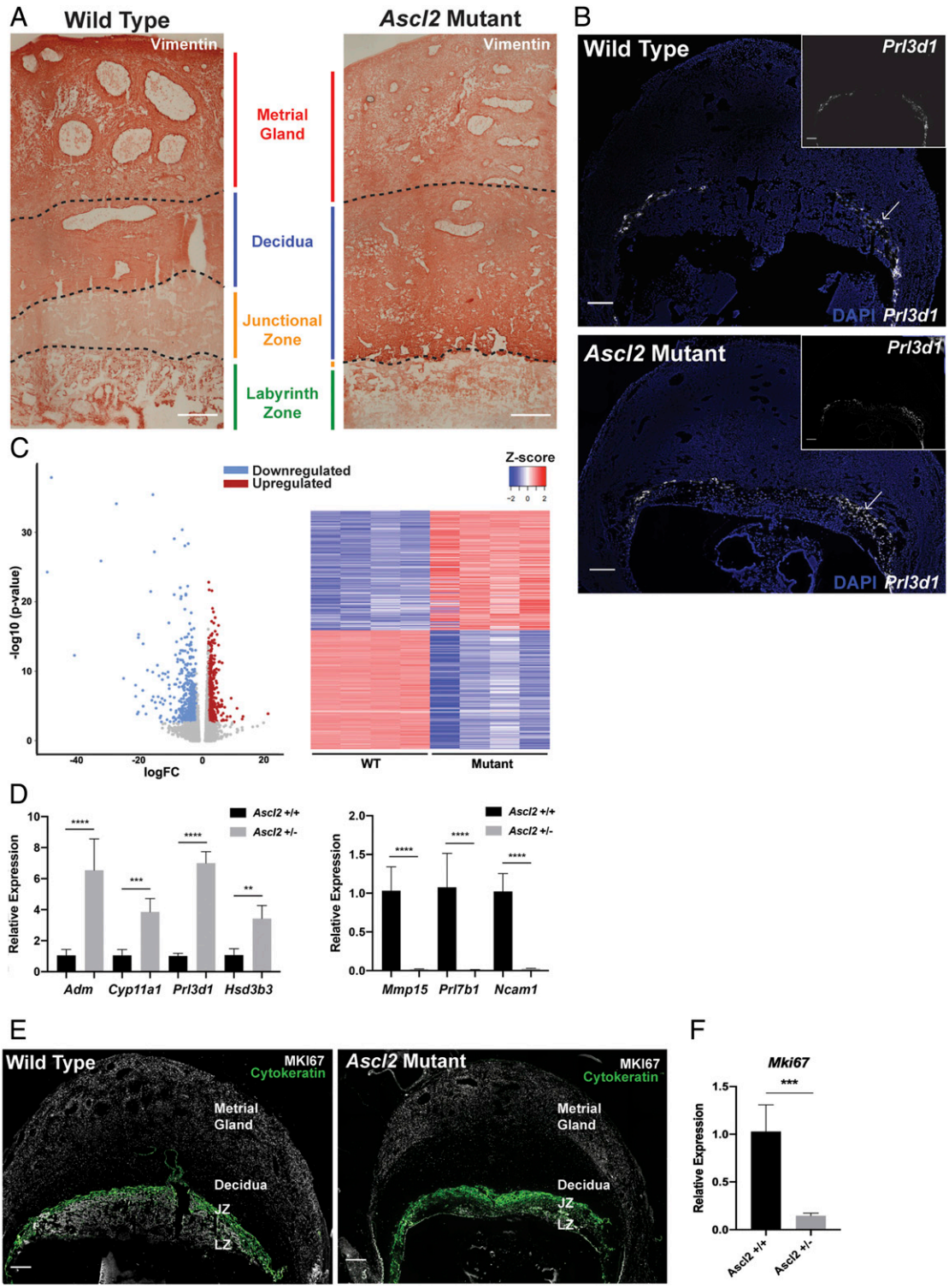

Fig. 4. *Ascl2* mutant placentation sites do not form an intact junctional zone. (*A*) Immunohistochemical analysis of vimentin in gd 12.5 WT and *Ascl2* mutant rat placentation sites. (*B*) In situ hybridization for *Prl3d1* (white) in gd 12.5 WT and Ascl2 mutant rat placentation sites. DAPI marks cell nuclei (blue). (*C*) Volcano plot and heat map depicting results of RNA-seq analysis from gd 12.5 placentas dissected from WT and *Ascl2* mutant (Mutant) specimens ($n = 4$ per group). The *x*-axis of the volcano plot depicts logarithm to base 2 of the fold change (logFC). Blue dots represent significantly down-regulated transcripts with $P \leq 0.05$ and a logarithm to base two-fold change of ≤ -2. Red dots represent significantly up-regulated transcripts with $P \leq 0.05$ and a logarithm to a base two-fold change of ≥ 2. The heat map depicts difference in gene expression between four WT and mutant samples. The heat map color key represents *z*-scores of RPKM values. (*D*) Validation of RNA-seq results by qRT-PCR confirms up-regulation of *Adm*, *Cyp11a1*, *Prl3d1*, and *Hsd3b3* and down-regulation of *Mmp15*, *Prl7b1*, and *Ncam1* in maternally inherited *Ascl2* mutant specimens (*Ascl2*$^{+/-}$; gray) compared with WT specimens (*Ascl2*$^{+/+}$; black). $n = 4$ per group. *$P < 0.05$; **$P < 0.01$; ***$P < 0.001$; ****$P < 0.0001$. All graphs depict mean ± SD values. (*E*) Immunohistochemical analyses of MKI67 (white) and cytokeratin (green) in gd 12.5 WT and *Ascl2* mutant rat placentation sites. (*F*) *Mki67* transcript levels are significantly decreased in gd 12.5 *Ascl2* mutant placentas compared with WT. $n = 4$. $P < 0.001$. (Scale bars, 500 μm.)

Downloaded at Palestinian Territory, occupied on December 11, 2021

www.manaraa.com

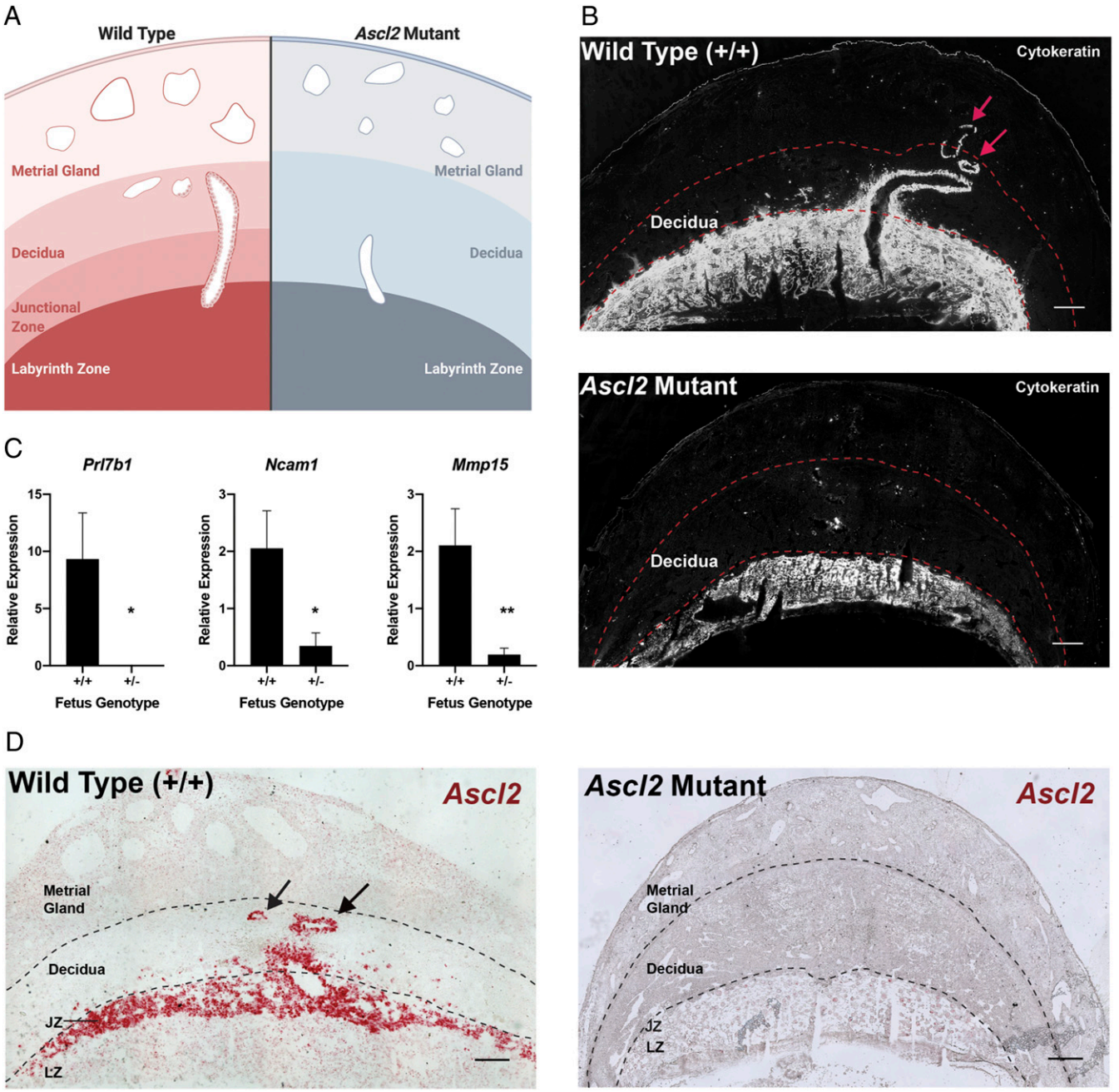

Fig. 5. Intrauterine trophoblast cell invasion is impaired in ASCL2-deficient placentation sites. (*A*) Schematic depicting the primary tissue zones comprising the rat placenta (BioRender). (*B*) Immunohistochemical analysis of cytokeratin (trophoblast marker) expression in gd 12.5 placentation sites from WT and *Ascl2* mutant specimens. Arrows indicate invasive endovascular trophoblast cells. (*C*) Relative expression of invasive trophoblast cell-specific transcripts *Prl7b1*, *Ncam1*, and *Mmp15* in dissected decidua tissue obtained from WT ($^{+/+}$) and maternally inherited *Ascl2* mutant ($^{+/-}$) placentation sites (WT, $n = 9$; mutant, $n = 10$). $^{*}P < 0.05$; $^{**}P < 0.01$. All graphs depict mean ± SEM values. (*D*) WT and *Ascl2* mutant rat placental tissue specimens obtained on gd 12.5 rats probed for *Ascl2* using in situ hybridization. *Ascl2* (red) is robustly expressed in the junctional zone and the invasive trophoblasts in the mesometrial decidua in WT, but not *Ascl2* mutant, placentation sites. The arrow indicates the location of invasive endovascular trophoblast cells. (Scale bars, 200 μm.)

alternatives for understanding hemochorial placentation. Using these research strategies, we have identified a regulator of hemochorial placentation with conserved actions. ASCL2 promotes invasive trophoblast cell development while antagonizing aspects of syncytiotrophoblast development.

ASCL2 is a conserved regulator of the invasive trophoblast cell lineage. Invasive trophoblast cells and their progenitors express ASCL2, and, importantly, disruption of ASCL2 impairs EVT cell differentiation from human TS cells and development of the invasive trophoblast cell lineage within the rat placentation site. EVT cells in humans arise from progenitor cells situated within the EVT cell column, whereas in the rat, the junctional zone serves a similar purpose. Understanding morphogenesis and cellular dynamics within the junctional zone provides insight into differentiation of the invasive trophoblast cell lineage in a physiological context. A number of genes have been implicated in the development of the junctional zone of the mouse placenta (e.g., *Ascl2*, *Egfr*, *Esx1*, *Phlda2*) (40); however, the connection of these

Downloaded at Palestinian Territory, occupied on December 11, 2021
www.manaraa.com

genes to the invasive trophoblast cell lineage has remained elusive, because intrauterine trophoblast cell invasion is rudimentary in the mouse (9). An exception was achieved through manipulating ASCL2 dosage in a mouse model, which implicated ASCL2 in the regulation of invasive glycogen trophoblast cells (19). Instead, mouse mutagenesis experiments have focused on endocrine and metabolic roles for the junctional zone (41, 42).

ASCL2 dosage has also been implicated in regulating the role of the junctional zone in modulating maternal metabolism (18). We propose that at least a subset of genes affecting junctional zone development will also impact the invasive trophoblast cell lineage, and that some of these genes will possess a conserved action, such as we have demonstrated for ASCL2. The origin of the invasive trophoblast cell lineage, including the identity of invasive trophoblast progenitor cells, their physical location within the junctional zone or earlier extraembryonic structures, their relationship with other trophoblast cell lineages, and the gene regulatory networks controlling their emergence, is yet to be defined.

ASCL2 interferes with the acquisition of syncytiotrophoblast phenotypic features in human trophoblast cell development. The human syncytiotrophoblast fate is highly specialized and includes unique hormone-producing capabilities that are not evident in rat or mouse syncytiotrophoblast (13). Among these endocrine activities is the biosynthesis of steroid hormones directed by members of the cytochrome P450 family (e.g., CYP11A1, CYP19A1) (43, 44). CYP19A1 (also called aromatase) is a key enzyme catalyzing the conversion of androgens to estrogens, a characteristic of human syncytiotrophoblast not evident in rodent syncytiotrophoblast (45–48). Consistent with our findings, Mendelson and colleagues previously showed that ASCL2 antagonizes CYP19A1 expression in human trophoblast cells (29, 30). Syncytiotrophoblast arise through the fusion of progenitors (49). Endogenous retroviral genes (*ERVW-1* and *ERVFRD-1*) encoding syncytins facilitate this key fusogenic event (50). The repressive actions of ASCL2 do not include repression of human syncytin gene expression. Thus, aspects of the human syncytiotrophoblast phenotype repressed by ASCL2 can be dissociated from trophoblast cell fusion. Strauss and colleagues made a similar determination using cyclic AMP to activate the "syncytiotrophoblast endocrine phenotype" prior to trophoblast fusion (51, 52).

Our observation of a reciprocal role of ASCL2 in trophoblast cell lineage development in the rat is not entirely consistent. We did not obtain any evidence supporting a role for ASCL2 affecting labyrinth zone or syncytiotrophoblast phenotypes in the *Ascl2* mutant rat model. Elucidation of such an in vivo role for ASCL2 may be confounded by the midgestation demise of the mutant placenta and embryo. Although there are many differences between the culture conditions and behaviors of human and rat TS cells, suppression of ASCL2 in both cell models activated genes associated with syncytiotrophoblast phenotypes. Thus, in vitro analyses support a conserved role for ASCL2 as a repressor of aspects of the syncytiotrophoblast phenotype.

We propose that establishment of the complete invasive/EVT cell program requires ASCL2 to act in a reciprocal manner. ASCL2 activates gene sets required for invasive/EVT cell development while repressing a subset of genes characteristic of a competing differentiated lineage, the syncytiotrophoblast. This set of actions is intriguing. Although ASCL2 may contribute to the regulation of a fundamental binary differentiation decision (i.e., invasive/EVT cells vs. syncytiotrophoblasts), the dosage of ASCL2 in differentiated EVT cells could also serve as a mechanism to instill functional plasticity, such as EVT cell acquisition of an endocrine phenotype. Heterogeneity of invasive trophoblast/EVT cell ASCL2 expression is compatible with such a proposal. The role of ASCL2 in trophoblast cell development is linked to both gene activation and repression, which could be direct or indirect. Direct actions would infer the assembly of distinct regulatory complexes at target genes, while indirect actions could involve an assortment of intermediaries. Collectively, these uncertainties are amenable to resolution with the in vitro and in vivo model systems that we have used for investigating the involvement of ASCL2 in trophoblast cell differentiation.

Materials and Methods

Human Placentation Site Specimens. Paraffin-embedded first trimester placental tissue specimens were obtained from the Lunenfeld-Tanenbaum Research Institute at Mount Sinai Hospital (Toronto, Canada) and were prepared from tissue specimens obtained from St. Mary's Hospital (Manchester, United Kingdom). Tissue collections were performed after written informed consent was obtained and on approval of the Human Research Ethics Review Committees at the University of Toronto, University of Manchester, and University of Kansas Medical Center (KUMC). All tissue samples were deidentified prior to use in these studies.

Animal Care and Treatment Specifications. Holtzman Sprague–Dawley rats were obtained from Envigo and maintained in an environmentally controlled facility with lights on from 0600 to 2000 h with free access to food and water as described previously (53). Virgin female rats (age 8 to 10 wk) were mated with adult male rats (age >3 mo). Mating was assessed by inspection of vaginal lavages; the presence of sperm in the vaginal lavage was designated gd 0.5. Rat placental tissues were collected from gd 11.5 to gd 20.5. Placentation sites were dissected into the placenta, overlying mesometrial decidua, uterine interface proximal to the mesometrial decidua (also referred to as the metrial gland), and junctional and labyrinth zone compartments, as described previously (11). Whole placentation sites were frozen in dry ice-cooled heptane for histologic and morphometric analyses. Dissected placentation site compartments were snap-frozen in liquid nitrogen and stored at −80 °C until processing for biochemical analyses. All rats were maintained in accordance with institutional policies for the care and use of vertebrate animals in research using protocols approved by the KUMC Animal Care and Use Committee.

Human TS Cell Culture. Human TS cells were maintained in stem state conditions or induced to differentiate into EVT cells or syncytiotrophoblast as described previously (34). Additional cell culture details are included in *SI Appendix*.

Rat TS Cell Culture. Blastocyst-derived rat TS cells (54) were cultured in rat TS cell medium (RPMI 1640, 20% [vol/vol] fetal bovine serum [FBS]; Thermo Fisher Scientific), 100 μm 2-mercaptoethanol (M7522; Sigma-Aldrich), 1 mM sodium pyruvate (11360-070, Thermo Fisher Scientific), 50 μM penicillin (15140122, Thermo Fisher Scientific), and 50 U/mL streptomycin (15140122, Thermo Fisher Scientific) supplemented with 70% rat embryonic fibroblast conditioned medium prepared as described previously (53, 54), fibroblast growth factor 4 (FGF4; 25 ng/mL, 100-31; Peprotech), and heparin (1 μg/mL, H3149; Sigma-Aldrich). For induction of differentiation, rat TS cells were cultured for 8 d in rat TS cell medium containing 1% (vol/vol) FBS and without FGF4 and heparin.

shRNA Construct Design and Lentivirus Production. shRNA constructs were obtained from Open Biosystems. *ASCL2* shRNAs were designed and subcloned into the pLKO.1 vector at AgeI and EcoRI restriction sites. shRNA sequences used in the analyses are included in *SI Appendix*, Table S1. Lentiviral packaging vectors were obtained from Addgene and included pMDLg/pRRE (plasmid 12251), pRSV-Rev (plasmid 12253), and pMD2.G (plasmid 12259). Lentiviral particles were produced following transient transfection of the shRNA-pLKO.1 vector and packaging plasmids into Lenti-X (632180; Takara Bio USA) cells using Attractene (301005; Qiagen) in Opti-MEM I (51985-034; Thermo Fisher Scientific). Cells were maintained in Dulbecco's Modified Eagle Medium (DMEM; 11995-065; Thermo Fisher Scientific) supplemented with 10% FBS until 24 h prior to supernatant collection, at which time the cells were cultured in basal human TS cell medium composed of DMEM/F12 (11320033; Thermo Fisher Scientific), 100 μm 2-mercaptoethanol, 0.2% (vol/vol) FBS, 50 μM penicillin, 50 U/mL streptomycin, 0.3% bovine serum albumin (BP9704100; Thermo Fisher Scientific), 1% (vol/vol) insulin-transferrin-selenium-ethanolamine solution (Thermo Fisher Scientific), 1.5 μg/mL L-ascorbic acid (A8960; Sigma-Aldrich), and 50 ng/mL epidermal growth factor (E9644; Sigma-Aldrich) for human TS cell transductions or rat TS cell medium for rat TS cell transductions. Supernatants were collected every 24 h for 2 d and stored frozen at −80 °C until use.

Lentiviral Transduction. Human TS cells were plated at 80,000 cells per well in 6-well tissue culture-treated plates coated with 5 μg/mL collagen IV

Downloaded at Palestinian Territory, occupied on December 11, 2021

www.manaraa.com

(CB40233; Thermo Fisher Scientific) and incubated for 24 h. Rat TS cells were plated at 100,000 cells per flask in T25 flasks and incubated for 24 h. Just before transduction, medium was changed, and cells were incubated with 2.5 μg/mL polybrene for 30 min at 37 °C. Immediately following polybrene incubation, TS cells were transduced with 500 μL (human) or 1,000 μL (rat) of lentiviral supernatant and then incubated for 24 h. Medium was changed at 24 h posttransduction and selected with puromycin dihydrochloride (5 μg/mL, A11138-03; Thermo Fisher Scientific) for 2 d. Cells recovered were cultured for 1 to 3 d in complete human TS medium before splitting for EVT cell differentiation or in rat TS cell medium prior to differentiation.

Transient Transfection. Human embryonic kidney-293T cells (Lenti-X 293T, 632180; Takara Bio USA) cells were transiently transfected with an ASCL2 (NM_005170) human c-Myc and DYKDDDDK (DDK) tagged open reading frame clone (RC209250; Origene) using Attractene (301005; Qiagen) in DMEM (11995-065; Thermo Fisher Scientific) supplemented with 10% FBS. Lysates were collected at 36 h and 48 h posttransfection.

Generation of an *Ascl2* Mutant Rat Model. A mutation at the rat *Ascl2* locus was generated using CRISPR/Cas9 genome editing. A gRNA targeting exon 2 of the *Ascl2* gene (gRNA: 5′-GGCUAGCGACGCGUGCCCUAGUUUUAGAGCUAUGCU-3′; NM_031503.2) was assembled with crRNA, tracrRNA, and Cas9 nuclease V3 (Integrated DNA Technologies). The genome editing constructs were electroporated into one-cell rat embryos using a NEPA21 electroporator (Bulldog Bio). The electroporated embryos were transferred to rat oviducts on day 0.5 of pseudopregnancy. Offspring were screened for mutations at specific target sites within the *Ascl2* gene by PCR, and the deletion was confirmed by DNA sequencing (GeneWiz). A founder animal possessing a 247-bp deletion within exon 2 was backcrossed with WT rats to evaluate germ line transmission. Phenotypic analyses were performed on offspring from intercrosses of heterozygous rats. Genotyping was performed by PCR (primers: 5′-GGGTGTTAATAGACCCCCAGA-3′, 5′-TTAAAAAGGAGCCGCTTGAG-3′, and 5′-GAAGTGGACGTTCGCACCTT-3′).

RNA Isolation, cDNA Synthesis, and qRT-PCR. Total RNA was isolated from cells and tissues with TRIzol reagent (15596018, Thermo Fisher Scientific) as described previously (53). cDNA was synthesized from 1 μg of total RNA using a High-Capacity cDNA Reverse Transcription Kit (4368813; Thermo Fisher Scientific) and diluted 10 times with water. qRT-PCR was performed using a reaction mixture containing PowerSYBR Green PCR Master Mix (4367659; Thermo Fisher Scientific) and primers (250 nM each). PCR primer sequences are presented in *SI Appendix*, Table S2. Amplification and fluorescence detection were carried out using a QuantStudio 7 Flex Real-Time PCR System (Thermo Fisher Scientific). An initial step (95 °C, 10 min) preceded 40 cycles of a two-step PCR at the following conditions: 92 °C, for 15 s and 60 °C for 1 min, followed by a dissociation step (95 °C for 15 s, 60 °C for 15 s, and 95 °C for 15 s). The comparative cycle threshold method was used for relative quantification of the amount of mRNA for each sample normalized to a housekeeping gene: *POLR2A* (human) or *Gapdh* (rat).

RNA-Seq Analysis. Transcript profiles were generated from control and ASCL2 knockdown CT27 human TS cells cultured in conditions promoting EVT cell differentiation ($n = 4$ experiments per group, including separate transductions) and from WT and ASCL2 mutant gd 12.5 rat placental tissue ($n = 4$ dams, or pooled tissues from four separate pregnancies per group). Complementary DNA libraries from total RNA samples were prepared with Illumina TruSeq RNA preparation kits according to the manufacturer's instructions. RNA integrity was assessed using an Agilent 2100 Bioanalyzer. Barcoded cDNA libraries were multiplexed onto a TruSeq paired-end flow cell and sequenced (100-bp paired-end reads) with a TruSeq 200-cycle SBS kit. Samples were run on an Illumina HiSeq 2500 sequencer at the Pediatric Genome Center at Children's Mercy or the KUMC Genome Sequencing Facility. Reads from *.fastq files were mapped to the human reference genome (GRCh37) and rat reference genome (Ensembl Rnor_5.0.78) using CLC Genomics Workbench 12.0 (Qiagen). Transcript abundance was expressed as reads per kilobase of transcript per million mapped reads (RPKM), and a false discovery rate of 0.05 was used as a cutoff for significant differential expression. Statistical significance was calculated by empirical analysis of digital gene expression followed by Bonferroni's correction.

Immunohistochemistry. Frozen placental tissues were sectioned at a thickness of 10 μm and incubated with 10% normal goat serum (50062Z; Thermo Fisher Scientific) for 1 h. Sections were incubated overnight with primary antibodies: pan cytokeratin (F3418; Sigma-Aldrich), vimentin (sc-6260; Santa Cruz Biotechnology), or MKI67 (ab16667; Abcam). After washing with phosphate-buffered saline (pH 7.4), sections were incubated for 2 h with corresponding secondary antibodies: Alexa Fluor 488-conjugated goat anti-mouse IgG (A32723; Thermo Fisher Scientific), Alexa Fluor 568-conjugated goat anti-rabbit IgG (A11011; Thermo Fisher Scientific), or rabbit anti-mouse IgG-peroxidase (A9044; Sigma-Aldrich). Nuclei were visualized with DAPI (Molecular Probes). Immunostained sections were mounted in Fluoromount-G (0100-01; SouthernBiotech) and imaged on a Nikon 80i upright microscope with a Photometrics CoolSNAP-ES monochrome camera (Roper).

Immunocytochemistry. Human TS cells were fixed with 4% paraformaldehyde (Sigma-Aldrich) for 20 min at room temperature. Immunocytochemical analysis was performed by immunofluorescence detection using a primary antibody against HLA-G (ab52455; Abcam), followed by Alexa Fluor 488-conjugated goat anti-mouse IgG (A32723; Thermo Fisher Scientific) secondary antibody and DAPI (Molecular Probes). Images were captured on a Nikon 80i upright microscope with a Roper Photometrics CoolSNAP-ES monochrome camera.

In Situ Hybridization. Detection of *ASCL2* transcripts was performed on paraffin-embedded human placenta tissue sections and fresh-frozen rat placenta tissue sections using the RNAscope 2.5 HD Reagent Kit (Advanced Cell Diagnostics), according to the manufacturer's instructions. Brightfield images were acquired on a Nikon 80i upright microscope with a Nikon Digital sight DS-Fi1 camera. Localization of *Ascl2*, *Prl7b1*, and *Prl3d1* transcripts was performed on fresh-frozen rat placentation sites. The RNAscope Fluorescent Multiplex Reagent Kit, version 2 (Advanced Cell Diagnostics) was used to colocalize transcripts. Probes were prepared by Advanced Cell Diagnostics to detect human *ASCL2* (311011, NM005170.2, target region: nucleotides 888 to 1,796), human *HLA-G* (426691-C2, NM_002127.5; target region: nucleotides 14 to 1,329), rat *Ascl2* (563011, NM_031503.2, target region: nucleotides 18 to 1,048), rat *Prl7b1* (860181-C2, NM_153738.1, target region: nucleotides 28 to 900), and rat *Prl3d1* (883661-C2, NM_017363.3). Fluorescence images were acquired on a Nikon 80i upright microscope with a Roper Photometrics CoolSNAP-ES monochrome camera.

Western Blot Analysis. Cell lysates were prepared by sonication in radioimmunoprecipitation assay lysis buffer (sc-24948A; Santa Cruz Biotechnology) supplemented with Halt protease and phosphatase inhibitor mixture (78443; Thermo Fisher Scientific). Protein concentrations were measured using the DC Protein Assay (5000113-115; Bio-Rad). Proteins were separated by sodium dodecyl sulfate polyacrylamide gel electrophoresis and transferred onto polyvinylidene difluoride membranes (10600023; GE Healthcare). After transfer, membranes were blocked with 5% nonfat milk in Tris-buffered saline with 0.1% Tween 20 (TBST) and probed with primary antibodies to DYKDDDDK Tag (1 μg/mL, 14793; Cell Signaling Technology), and glyceraldehyde-3-phosphate dehydrogenase (ab9485; Abcam) overnight at 4 °C. Membranes were washed three times for 5 min with TBST and then incubated with secondary antibodies (goat anti-rabbit IgG HRP, A0545; Sigma Aldrich and goat anti-mouse IgG HRP, 7076; Cell Signaling Technology) for 1 h at room temperature. Immunoreactive proteins were visualized using Luminata Crescendo Western HRP Substrate (WBLUR0500; Millipore Sigma) according to the manufacturer's instructions.

Statistical Analysis. Statistical analyses were performed with GraphPad Prism 9 software. Welch's *t* tests, Brown–Forsythe and Welch ANOVA, or two-way ANOVA were applied as appropriate. Statistical significance was determined as $P < 0.05$.

Data Availability. The datasets generated and analyzed for this study have been deposited in the Gene Expression Omnibus (GEO) database, https://www.ncbi.nlm.nih.gov/geo/ (accession no. GSE154350).

ACKNOWLEDGMENTS. We thank Stacy Oxley, Priscilla Nechrebecki, and Brandi Miller for their assistance. We also thank the staff of the University of Kansas Medical Center Laboratory Animal Resources and Sarah Tague, PhD, at the Kansas Intellectual and Developmental Disabilities Research Center Imaging Core Facility which is supported by grants from the NIH (NIH U54, HD090216). This research was supported by a National Research Service Award postdoctoral fellowship from the NIH (F32HD096809, to K.M.V) and grants from the NIH (HD020676, HD079363, and HD099638) and the Sosland Foundation.

Downloaded at Palestinian Territory, occupied on December 11, 2021

www.manaraa.com

1. R. Pijnenborg, L. Vercruysse, M. Hanssens, The uterine spiral arteries in human pregnancy: Facts and controversies. *Placenta* **27**, 939–958 (2006).
2. P. Velicky, M. Knöfler, J. Pollheimer, Function and control of human invasive trophoblast subtypes: Intrinsic vs. maternal control. *Cell Adhes. Migr.* **10**, 154–162 (2016).
3. R. Ain, L. N. Canham, M. J. Soares, Gestation stage-dependent intrauterine trophoblast cell invasion in the rat and mouse: Novel endocrine phenotype and regulation. *Dev. Biol.* **260**, 176–190 (2003).
4. M. Bilban *et al*., Trophoblast invasion: Assessment of cellular models using gene expression signatures. *Placenta* **31**, 989–996 (2010).
5. I. Brosens, R. Pijnenborg, L. Vercruysse, R. Romero, The "Great Obstetrical Syndromes" are associated with disorders of deep placentation. *Am. J. Obstet. Gynecol.* **204**, 193–201 (2011).
6. M. Gormley *et al*., Preeclampsia: Novel insights from global RNA profiling of trophoblast subpopulations. *Am. J. Obstet. Gynecol.* **217**, 200.e1–200.e17 (2017).
7. S. L. Adamson *et al*., Interactions between trophoblast cells and the maternal and fetal circulation in the mouse placenta. *Dev. Biol.* **250**, 358–373 (2002).
8. P. M. Coan, N. Conroy, G. J. Burton, A. C. Ferguson-Smith, Origin and characteristics of glycogen cells in the developing murine placenta. *Dev. Dyn.* **235**, 3280–3294 (2006).
9. R. Pijnenborg, L. Vercruysse, "Animal models of deep trophoblast invasion" in *Placental Bed Disorders: Basic Science and its Translation to Obstetrics*, R. Pijnenborg, I. Brosens, R. Romero, Eds. (Cambridge University Press, 2010), pp. 127–139.
10. M. J. Soares, D. Chakraborty, M. A. Karim Rumi, T. Konno, S. J. Renaud, Rat placentation: An experimental model for investigating the hemochorial maternal-fetal interface. *Placenta* **33**, 233–243 (2012).
11. R. Ain, T. Konno, L. N. Canham, M. J. Soares, Phenotypic analysis of the rat placenta. *Methods Mol. Med.* **121**, 295–313 (2006).
12. M. J. Soares *et al*., Differentiation of trophoblast endocrine cells. *Placenta* **17**, 277–289 (1996).
13. M. J. Soares, K. M. Varberg, K. Iqbal, Hemochorial placentation: Development, function, and adaptations. *Biol. Reprod.* **99**, 196–211 (2018).
14. F. Guillemot, A. Nagy, A. Auerbach, J. Rossant, A. L. Joyner, Essential role of Mash-2 in extraembryonic development. *Nature* **371**, 333–336 (1994).
15. M. Tanaka, M. Gertsenstein, J. Rossant, A. Nagy, Mash2 acts cell autonomously in mouse spongiotrophoblast development. *Dev. Biol.* **190**, 55–65 (1997).
16. R. Oh *et al*., Epigenetic and phenotypic consequences of a truncation disrupting the imprinted domain on distal mouse chromosome 7. *Mol. Cell. Biol.* **28**, 1092–1103 (2008).
17. R. Oh-McGinnis, A. B. Bogutz, L. Lefebvre, Partial loss of Ascl2 function affects all three layers of the mature placenta and causes intrauterine growth restriction. *Dev. Biol.* **351**, 277–286 (2011).
18. S. J. Tunster, G. I. McNamara, H. D. J. Creeth, R. M. John, Increased dosage of the imprinted Ascl2 gene restrains two key endocrine lineages of the mouse placenta. *Dev. Biol.* **418**, 55–65 (2016).
19. A. B. Bogutz *et al*., Transcription factor ASCL2 is required for development of the glycogen trophoblast cell lineage. *PLoS Genet.* **14**, e1007587 (2018).
20. J. Rossant *et al*., Mash2 is expressed in oogenesis and preimplantation development but is not required for blastocyst formation. *Mech. Dev.* **73**, 183–191 (1998).
21. M. Tanaka *et al*., Parental origin-specific expression of Mash2 is established at the time of implantation with its imprinting mechanism highly resistant to genome-wide demethylation. *Mech. Dev.* **87**, 129–142 (1999).
22. F. Guillemot *et al*., Genomic imprinting of Mash2, a mouse gene required for trophoblast development. *Nat. Genet.* **9**, 235–242 (1995).
23. M. R. W. Mann *et al*., Selective loss of imprinting in the placenta following preimplantation development in culture. *Development* **131**, 3727–3735 (2004).
24. L. Lefebvre *et al*., The interval between Ins2 and Ascl2 is dispensable for imprinting centre function in the murine Beckwith-Wiedemann region. *Hum. Mol. Genet.* **18**, 4255–4267 (2009).
25. M. J. Janatpour *et al*., A repertoire of differentially expressed transcription factors that offers insight into mechanisms of human cytotrophoblast differentiation. *Dev. Genet.* **25**, 146–157 (1999).
26. B. A. Westerman *et al*., The Human Achaete Scute Homolog 2 gene contains two promotors, generating overlapping transcripts and encoding two proteins with different nuclear localization. *Placenta* **22**, 511–518 (2001).
27. G. Meinhardt, P. Husslein, M. Knöfler, Tissue-specific and ubiquitous basic helix-loop-helix transcription factors in human placental trophoblasts. *Placenta* **26**, 527–539 (2005).
28. A. K. Wakeland *et al*., Hypoxia directs human extravillous trophoblast differentiation in a hypoxia-inducible factor-dependent manner. *Am. J. Pathol.* **187**, 767–780 (2017).
29. B. Jiang, C. R. Mendelson, USF1 and USF2 mediate inhibition of human trophoblast differentiation and CYP19 gene expression by Mash-2 and hypoxia. *Mol. Cell. Biol.* **23**, 6117–6128 (2003).
30. B. Jiang, A. Kamat, C. R. Mendelson, Hypoxia prevents induction of aromatase expression in human trophoblast cells in culture: Potential inhibitory role of the hypoxia-inducible transcription factor Mash-2 (Mammalian Achaete-Scute Homologous Protein-2). *Mol. Endocrinol.* **14**, 1661–1673 (2000).
31. Y. Liu *et al*., Single-cell RNA-seq reveals the diversity of trophoblast subtypes and patterns of differentiation in the human placenta. *Cell Res.* **28**, 819–832 (2018).
32. R. Vento-Tormo *et al*., Single-cell reconstruction of the early maternal-fetal interface in humans. *Nature* **563**, 347–353 (2018).
33. D. O. Wiemers, R. Ain, S. Ohboshi, M. J. Soares, Migratory trophoblast cells express a newly identified member of the prolactin gene family. *J. Endocrinol.* **179**, 335–346 (2003).
34. H. Okae *et al*., Derivation of human trophoblast stem cells. *Cell Stem Cell* **22**, 50–63.e6 (2018).
35. C. Lavialle *et al*., Paleovirology of "syncytins," retroviral env genes exapted for a role in placentation. *Philos. Trans. R. Soc. Lond. B Biol. Sci.* **368**, 20120507 (2013).
36. Y. Abbas, M. Y. Turco, G. J. Burton, A. Moffett, Investigation of human trophoblast invasion in vitro. *Hum. Reprod. Update* **26**, 501–513 (2020).
37. M. Horii, O. Touma, T. Bui, M. M. Parast, Modeling human trophoblast, the placental epithelium at the maternal fetal interface. *Reproduction* **160**, R1–R11 (2020).
38. C. Q. E. Lee *et al*., What is trophoblast? A combination of criteria define human first-trimester trophoblast. *Stem Cell Reports* **6**, 257–272 (2016).
39. J. K. Cinkornpumin *et al*., Naive human embryonic stem cells can give rise to cells with a trophoblast-like transcriptome and methylome. *Stem Cell Reports* **15**, 198–213 (2020).
40. L. Woods, V. Perez-Garcia, M. Hemberger, Regulation of placental development and its impact on fetal growth—new insights from mouse models. *Front. Endocrinol. (Lausanne)* **9**, 570 (2018).
41. R. M. John, Epigenetic regulation of placental endocrine lineages and complications of pregnancy. *Biochem. Soc. Trans.* **41**, 701–709 (2013).
42. S. J. Tunster, B. Tycko, R. M. John, The imprinted Phlda2 gene regulates extraembryonic energy stores. *Mol. Cell. Biol.* **30**, 295–306 (2010).
43. E. D. Albrecht, G. J. Pepe, Placental steroid hormone biosynthesis in primate pregnancy. *Endocr. Rev.* **11**, 124–150 (1990).
44. W. L. Miller, R. J. Auchus, The molecular biology, biochemistry, and physiology of human steroidogenesis and its disorders. *Endocr. Rev.* **32**, 81–151 (2011).
45. G. Gibori *et al*., Placental-derived regulators and the complex control of luteal cell function. *Recent Prog. Horm. Res.* **44**, 377–429 (1988).
46. E. R. Simpson *et al*., Aromatase expression in health and disease. *Recent Prog. Horm. Res.* **52**, 185–213, discussion 213–214 (1997).
47. M. Ben-Zimra *et al*., Uterine and placental expression of steroidogenic genes during rodent pregnancy. *Mol. Cell. Endocrinol.* **187**, 223–231 (2002).
48. A. Kamat, M. M. Hinshelwood, B. A. Murry, C. R. Mendelson, Mechanisms in tissue-specific regulation of estrogen biosynthesis in humans. *Trends Endocrinol. Metab.* **13**, 122–128 (2002).
49. H. J. Kliman, J. E. Nestler, E. Sermasi, J. M. Sanger, J. F. Strauss, 3rd, Purification, characterization, and in vitro differentiation of cytotrophoblasts from human term placentae. *Endocrinology* **118**, 1567–1582 (1986).
50. A. Dupressoir, C. Lavialle, T. Heidmann, From ancestral infectious retroviruses to bona fide cellular genes: Role of the captured syncytins in placentation. *Placenta* **33**, 663–671 (2012).
51. M. A. Feinman, H. J. Kliman, S. Caltabiano, J. F. Strauss, 3rd, 8-Bromo-3′,5′-adenosine monophosphate stimulates the endocrine activity of human cytotrophoblasts in culture. *J. Clin. Endocrinol. Metab.* **63**, 1211–1217 (1986).
52. J. F. Strauss, 3rd, S. Kido, R. Sayegh, N. Sakuragi, M. E. Gåfvels, The cAMP signalling system and human trophoblast function. *Placenta* **13**, 389–403 (1992).
53. J. Nteeba *et al*., Poorly controlled diabetes mellitus alters placental structure, efficiency, and plasticity. *BMJ Open Diabetes Res. Care* **8**, e001243 (2020).
54. K. Asanoma *et al*., FGF4-dependent stem cells derived from rat blastocysts differentiate along the trophoblast lineage. *Dev. Biol.* **351**, 110–119 (2011).

Downloaded at Palestinian Territory, occupied on December 11, 2021

www.manaraa.com